Sound & Vibration 2026, 60(4), 4345.
doi: https://doi.org/10.59400/sv4345

Article

Influence of spruce guitar resonance panel structure on acoustic vibration response characteristics

Guanzheng Wan, Jinyi Chen, Yihang Ben, Siyuan Wang, Liang Zhang, Lan He, Yuanji Zhao, Haotian Cui, Zhenbo Liu*

Key Laboratory of Bio-Based Material Science & Technology of Ministry of Education, Northeast Forestry University, Harbin 150040, China
*** Corresponding author:** Zhenbo Liu, liu.zhenbo@foxmail.com

CITATION

Wan G, Chen J, Ben Y, et al. Influence of spruce guitar resonance panel structure on acoustic vibration response characteristics. Sound & Vibration. 2026; 60(4): 4345. https://doi.org/10.59400/sv4345

ARTICLE INFO

Received: 30 April 2026
Revised: 21 May 2026
Accepted: 27 May 2026
Available online: 22 July 2026

Abstract: In recent years, the guitar manufacturing industry has faced a growing shortage of large-diameter, high-quality spruce wood resources. To address this issue, it is urgently necessary to conduct research on the structural design of guitar resonance panels. This study investigates three types of spruce guitar resonance panels with different structures, exciting them at various points, and using a multi-channel FFT analyzer to capture vibration signals and analyze their acoustic vibration response characteristics. The results show that in terms of root mean square (RMS) values indicating overall signal intensity and peak-to-peak values reflecting signal amplitude, the double-spliced resonance panel exhibits the highest vibration energy, followed by the quadruple-spliced resonance panel, while the triple-spliced resonance panel shows the lowest. Regarding spectral centroid and high-frequency energy—indicating richness of high-frequency content—and spectral flatness and kurtosis—reflecting uniformity of energy distribution—the triple-spliced resonance panel demonstrates the brightest tonal quality and the most even spectral energy distribution, followed by the quadruple-spliced panel. From raw material to finished panel, and from double-spliced to quadruple-spliced panels, both elastic modulus and shear modulus show an increasing trend. Compared to the double-spliced panel, multi-spliced panels exhibit higher specific dynamic elastic modulus and acoustic impedance, but lower acoustic radiation quality constant. Although individual parameters vary to some extent, the overall acoustic vibration performance of multi-spliced panels differs little from that of the double-spliced panel. These findings not only provide practical guidance for manufacturers but also offer theoretical support for improving the acoustic quality of guitars.

Keywords: guitar resonance panels; peak-to-peak value; root mean square; spectral centroid; high-frequency energy; acoustic vibration performance

1. Introduction

Music plays a role in cultivating character and fostering noble interests, and instruments are an important medium in music education [1]. The guitar is a widely used musical instrument. In the process of guitar making, the resonance panel is extremely important in the design of the sound box. Since the resonance panel needs to respond quickly to the vibration of the strings, it should be relatively light. However, as it needs to withstand a certain amount of tension, it should also have good toughness and strength [2]. In terms of materials, although some researchers have attempted to use composite materials or subject low-cost wood to physical/chemical treatments to replace the resonance panels of stringed instruments, they still fall short in acoustic performance compared to high-quality wood used for musical instruments [3–6]. Therefore, the main material for guitar resonance panels remains natural wood used for musical instruments, as this type of wood has excellent acoustic properties [7, 8]. Makers usually use high-quality woods such as red pine, Sitka spruce, and European spruce as resonance panel materials. Structurally, guitar resonance panels are mainly divided into solid single boards and plywood. Plywood uses artificial laminated wood. Since plywood is made by gluing multiple layers of wood together, it has the characteristics of structural stability and easier preservation [9], but it is inferior to solid single boards in terms of acoustic vibration performance. Solid single boards are classified as double-spliced and quadruple-spliced resonance panels based on the number of materials (structures). A double-spliced resonance panel is made by cutting a 10 mm thick radially cut board along the center line into two 5 mm thick thin boards, then gluing and sanding them together [10]. It has only one central glue seam, good symmetry, and less scattering of bending waves, which can better maintain the acoustic vibration characteristics of spruce [11], but it requires large-diameter high-quality spruce logs. A triple-spliced resonance panel is made by gluing three boards together, with two glue seams. A quadruple-spliced resonance panel is made by gluing four boards together with three parallel glue seams, which can improve the utilization rate of wood. Currently, most guitar manufacturers mainly use the double-spliced resonance panel process, with a small number of manufacturers adopting the quadruple-spliced resonance panel process. However, the double-spliced resonance panel is still the most recognized by the mainstream consumer group. The quadruple-spliced resonance panel differs from the double-spliced one in both process and structure. Due to the production process, compared to the triple-spliced and quadruple-spliced resonance panels, the double-spliced resonance panel requires larger diameter logs to be cut. However, as spruce has a long growth cycle (ranging from several decades to over a hundred years), the resources of large-diameter spruce wood are gradually becoming scarce. To effectively utilize and protect forest resources, it is necessary to study the acoustic vibration conditions of resonance panels with more than two materials and make comparisons to identify the corresponding influencing factors.

Research shows that the material, shape, and size, structure, and physical properties of the resonance panel of musical instruments have a significant impact on the acoustic vibration performance of the panel [12, 13]. The guitar resonance panel is relatively large, with a maximum width of approximately 300 mm and a maximum length of about 500 mm. The thickness of the panel after grinding and processing is generally between 2 and 4 mm, which can be regarded as a wooden thin plate. This large size makes it difficult to conduct traditional acoustic vibration performance tests on the guitar resonance panel during production. In previous studies, specimens were often cut into beam shapes for the determination of acoustic vibration performance, which has a significant difference from the actual shape and size of the panel, and the vibration mode of the beam-shaped specimen is also different from that of the actual-sized panel. When determining the acoustic response of the beam-shaped specimen by the resonance method, the beam mainly undergoes bending vibration, and the torsional vibration can be ignored. However, in the vibration process of the guitar resonance panel, both bending vibration and torsional vibration usually participate simultaneously, and the vibration components are quite complex, making it difficult to quickly identify each resonant frequency and distinguish the vibration type corresponding to that frequency. At the same time, when determining the acoustic response of wooden thin plates, boundary conditions, excitation positions, and other factors also have a significant impact on the acoustic response of the specimen. The guitar resonance panel without cutting out the guitar contour can be regarded as a rectangular thin plate, and the vibration characteristics of the panel can be solved by applying the vibration theory of anisotropic rectangular thin plates.

Previous research on the structure of the resonance panel of stringed instruments such as guitars has mainly focused on three aspects:

1. The influence of the thickness and distribution of the resonance panel on the acoustic vibration characteristics [14–16]. It was found that the thickness distribution of the resonance panel significantly affects its natural frequency and modal shape, and the uniform thinning of the panel leads to a proportional decrease in all modal frequencies.
2. The influence of additional structures on the resonance panel on the acoustic vibration characteristics [17,18]. Studies have shown that additional structures not only affect the modal frequency and shape of the resonance panel but also interact with the stiffness characteristics of other parts of the instrument after assembly, significantly altering the overall vibration response.
3. Establishing a finite element model to predict the influence of structural changes on the acoustic vibration characteristics of the resonance panel [19–22], and verifying the reliability of the model through experimental results. Existing research on the variable of the jointing process is still relatively weak, mostly focusing on the influence of the shape and thickness of the resonance panel on the acoustic vibration characteristics, or only paying attention to the influence of the glue joint on the static performance, while lacking in-depth exploration of the mechanism of the glue joint in the propagation of sound waves and the superposition effect of multiple glue joints.

This study takes the spruce guitar resonance panel (a rectangular blank without the guitar outline cut out) as the research object. Through experiments, it explores the influence of the law of structural changes (double, triple, and quadruple splicing) on the acoustic vibration response characteristics of the resonance panel, reveals the mechanism of the effect of the glue joint on its acoustic vibration response characteristics, and provides a scientific basis for the panel process decision-making of guitar enterprises under the background of the shortage of high-quality large-diameter spruce resources.

2. Materials and methods

2.1. Test materials

The specific experimental materials used in this study are: European spruce (Picea abies) wood, with an air-dry density of 0.45–0.5 $g{\cdot}cm^{-3}$, uniform annual ring width, smooth surface, clear texture, and no knots, cracks, or wormholes. The wood was purchased from Qingdao Hongyue Musical Instruments Co., Ltd. Due to the extreme scarcity worldwide of exceptionally large, high-quality quarter-sawn spruce logs capable of meeting the width requirements for premium instrument soundboards, the use of solid, full-width boards in mass production has become nearly nonexistent in modern guitar and piano manufacturing, limited by the natural width of available logs. This study uses the double-spliced resonance panel—the most widely applied and acoustically recognized superior type in the industry, constructed by splitting a 10 mm thick quarter-sawn board along its centerline into two 5 mm thick thin plates and then mirror-gluing them together—as the baseline control for this experiment. Six test samples were used for each type of guitar soundboard (double-spliced, triple-spliced, quadruple-spliced). The basic parameters are shown in **Table 1**. To ensure the reliability of the experiment and minimize errors caused by the inherent differences in the experimental materials, the resonance panels used in this study were selected from the same origin, batch, and grade of European spruce wood, with similar straightness and width of the grain, all parallel to the length direction, and processed and stored under the same conditions. The triple-spliced resonance panel and quadruple-spliced resonance panel are sequentially processed from the double-spliced resonance panel, ensuring high consistency in the wood grain structure among the three types of specimens. All specimens were subjected to identical drying, sanding, bonding, and curing conditions, with consistent adhesive type and glue application amount maintained throughout. The processing flow is shown in **Figure 1**.

Table 1. Basic parameters of the test specimen.

Specimen category	L/cm	R/cm	T/cm	ρ/g·cm^{-3}
Double-spliced resonance panel material	56.25	22.12	0.51	0.463
Double-spliced resonance panel	56.20	43.72	0.38	0.480
Triple-spliced resonance panel material specification 1	55.98	21.89	0.38	0.493
Triple-spliced resonance panel material specification 2	56.01	10.89	0.38	0.495
Triple-spliced resonance panel	56.03	42.77	0.29	0.497
Quadruple-spliced resonance panel material	56.02	10.50	0.29	0.496
Quadruple-spliced resonance panel	55.99	40.31	0.23	0.505

Note: The resonance panel is made by splicing the panel materials in the horizontal direction, and the Triple-spliced resonance panel is made by splicing two types of panel materials with different widths.

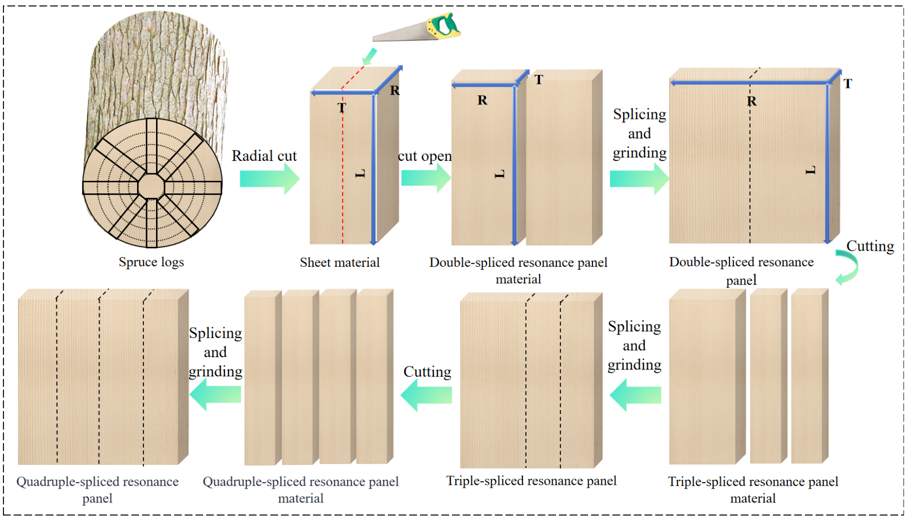

Figure 1. Flowchart of specimen processing.

2.2. Test methods

2.2.1. Principles and methods of materials testing

All the resonance panel materials of spruce are long and narrow boards, and their length and width are much greater than their thickness. The dynamic elastic modulus can be determined by the Euler beam method, and then the acoustic vibration parameters can be obtained .

$$E = \frac{48\pi^2 \rho a^4 f_b^2}{\beta^4 h^2} \tag{1}$$

In the formula, E represents the dynamic elastic modulus of the specimen, in Pa; a, b, and h are the length, width, and thickness of the specimen, respectively, in m; ρ is the density, in kg/m^3; f_b is the first-order bending frequency of the plate's free vibration, in Hz; β is a constant related to the boundary conditions, and it takes the value of 4.73 for the first-order vibration.

The test system is shown in **Figure 2**. The specimen is supported by a triangular bracket at the first-order nodal line (0.224 L from both ends). As the specimen is relatively thin, a wooden stick is used to strike the end of the specimen to generate excitation and induce free vibration. The vibration signal collected by the microphone is transmitted to a multi-channel fast Fourier transform (FFT) analyzer (ONO SOKKI, CF5220Z), from which the discrete time-domain and frequency-domain signals of the specimen's vibration are obtained.

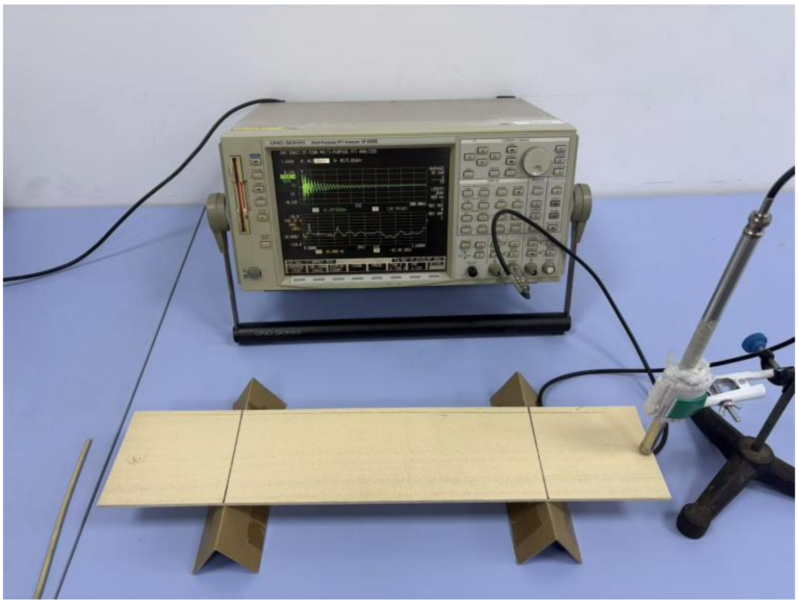

Figure 2. Testing system.

Considering that the shape of the spruce guitar resonance panel is regular and its length and width are much greater than its thickness, the spruce resonance panel can be regarded as a rectangular thin plate for measurement . Also, since the spruce resonance panel is a wooden material and belongs to an anisotropic material, the vibration theory of anisotropic rectangular thin plates can be applied [23]. The vibration characteristics of the spruce resonance panel are solved. The differential equation of the transverse free vibration of orthotropic thin plates is:

$$D_{11}\frac{\partial^4 w}{\partial x^4}+2(D_{12}\ \ +2D_{66})\frac{\partial^4 w}{\partial x^2\partial y^2}+D_{22}\frac{\partial^4 w}{\partial y^4}-\frac{\rho\omega^2}{g}w=0 \tag{2}$$

In the formula, D_{11}, D_{12}, and D_{22} represent the bending stiffnesses in different directions; D_{66} represents the torsional stiffness; w represents the deflection; and ρ represents the density.

For anisotropic wooden thin plates, the Rayleigh method can be used to solve the differential equation of transverse free vibration of orthotropic thin plates, and the frequency equation of free vibration of wooden thin plates can be obtained:

$$f_{(m,n)}=\frac{1}{2\pi}\sqrt{\frac{D_{11}\frac{\alpha_{1(m,n)}}{a^4}+D_{22}\frac{\alpha_{2(m,n)}}{b^4}+2D_{12}\frac{\alpha_{3(m,n)}}{a^2b^2}+4D_{66}\frac{\alpha_{4(m,n)}}{a^2b^2}}{\rho\mathrm{h}}} \tag{3}$$

In the formula, $f(m,\ n)$ represents the frequency corresponding to the (m, n) mode shape, in Hz; a, b, and h are the length, width, and thickness of the specimen, respectively, in m; ρ is the density, in kg/m^3. The constant coefficients $\alpha_{1(m,n)}$, $\alpha_{2(m,n)}$, $\alpha_{3(m,n)}$, and $\alpha_{4(m,n)}$ of the free vibration frequency equation for wooden thin plates can be obtained from **Table 2** [24].

Table 2. Constant coefficient α (m, n) of the free vibration frequency equation for wooden thin plates.

(*m*, *n*)	**α₁**	**α₂**	**α₃**	**α₄**
(1,1)	0	0	0	144
(0,2)	0	500.6	0	0
(2,0)	500.6	0	0	0
(*m*,0)	γ^4	0	0	0
(0,*n*)	0	ε^4	0	0

Note: When m and n are greater than 2, $\gamma = (m-0.5)$, $\varepsilon = (n-0.5)$.

By solving and simplifying formula (3), formulas (4) to (7) for calculating the dynamic elastic modulus and dynamic shear modulus can be obtained:

$$E_x=\frac{12}{h^3}D_{11}(1-\mu_x\mu_y) \tag{4}$$

$$E_y=\frac{12}{h^3}D_{22}(1-\mu_x\mu_y) \tag{5}$$

$$G=\frac{12}{h^3}D_{66} \tag{6}$$

$$D_{12}=\frac{\sqrt{E_xE_y\mu_x\mu_y}}{12(1-\mu_x\mu_y)}h^3 \tag{7}$$

Based on the constant coefficient table and formulas (4) to (7), further simplification can be achieved to obtain formulas (8) to (13).

$$E_x=\frac{48\pi^2\rho a^4 f_{(2,0)}^{\,2}}{500.6h^2}(1-\mu_x\mu_y) \tag{8}$$

$$E_y = \frac{48\pi^2 \rho b^4 f_{(0,2)}^2}{500.6h^2}(1 - \mu_x \mu_y) \tag{9}$$

$$G = \frac{48\pi^2 \rho a^2 b^2 f_{(1,1)}^2}{576h^2} \tag{10}$$

$$f_{(m,\,0)} = \sqrt{\frac{\gamma^4 E_x}{48\pi^2 \rho a^4 (1 - \mu_x \mu_y)}}\ h \tag{11}$$

$$f_{(0,\,n)} = \sqrt{\frac{\varepsilon^4 E_y}{48\pi^2 \rho b^4 (1 - \mu_x \mu_y)}}\ h \tag{12}$$

$$f_{(1,\,1)} = \sqrt{\frac{12G}{\pi^2 \rho a^2 b^2}}\ h \tag{13}$$

In the formula, E_x and E_y represent the dynamic elastic modulus, in Pa; G represents the dynamic shear modulus, in Pa; $(1- \mu_x\mu_y)$ is usually taken as 0.99 [25].

From the above, it can be seen that by measuring the frequencies corresponding to the (2,0), (0,2), and (1,1) vibration modes of the specimen, the dynamic elastic modulus and dynamic shear modulus of the guitar resonance panel sample can be determined [26].

The vibration of the resonance panel is rather complex. To accurately measure the vibration frequencies of each order of the panel, the elastic line suspension method and multi-point excitation approach are adopted. This study employs a rectangular light panel as a simplified model, aiming to eliminate the interference of guitar contour geometry and focus on the impact of structural variations on the acoustic vibration characteristics of the resonance panel. Therefore, the selection of excitation points does not simulate the actual guitar bridge position but is based on two principles: first, investigating the relative relationship between the excitation point and the wood grain direction as well as the glue joint direction; second, ensuring effective excitation of specific modal frequencies of the resonance panel. The free vibration measurement system of the panel and the positions of the excitation points are shown in **Figure 3** (represents the excitation position and × represents the microphone position). The sample is suspended by elastic ropes (in the figure, it is suspended at the intersection of the center lines of the sample's length and width). The positions of the microphones and excitation points are determined based on the expected vibration modes [26]. The resonance panel coordinate system has its origin (0,0) at the geometric center of the panel, with the positive X-axis pointing horizontally to the right (along the length of the panel, i.e., the longitudinal direction of the wood), and the positive Y-axis pointing vertically upward (along the width of the panel, i.e., the radial direction of the wood). The panel is approximately 560 mm in length and 420 mm in width, resulting in (9, 2): [(−280, −210), (280, 210)], (6, 5): [(−280, 0), (280, 0)], and (3, 8): [(0, 210),(0, −210)]. The specific excitation point positions are as follows: (9, 2) position: The excitation position and the microphone position are at the two ends of one diagonal of the sample, which can highlight the (1, 1) order frequency. (6, 5) position: The excitation position and the microphone position are at the two ends of the center line of the sample's width (in the direction of the grain), which can highlight the (2, 0) order frequency.

(3, 8) position: The excitation position and the microphone position are at the two ends of the center line of the sample's length (in the direction perpendicular to the grain), which can highlight the (0, 2) order frequency. A light tap is used to apply excitation, causing the sample to vibrate freely. The microphone transmits the collected signal to a dual-channel fast Fourier transform (FFT) analyzer (ONO SOKKI, CF5220Z), obtaining the time-domain and frequency-domain graphs of the sample's vibration. The resonant frequencies of each order are identified and calculated respectively according to the formula. For rectangular thin plates, when the excitation point varies within a small local range (e.g., ±10 mm), the measured frequency response function shows minimal changes in peak frequencies for low-frequency modes (<500 Hz), with only slight amplitude fluctuations observed near higher-order modes or nodal points. In this experiment, we carefully marked the excitation positions to ensure repeatability within ±5 mm, maintained consistent excitation force as much as possible, applied five repeated excitations at each position to reduce random errors by taking averages, and conducted multiple repeated tests.

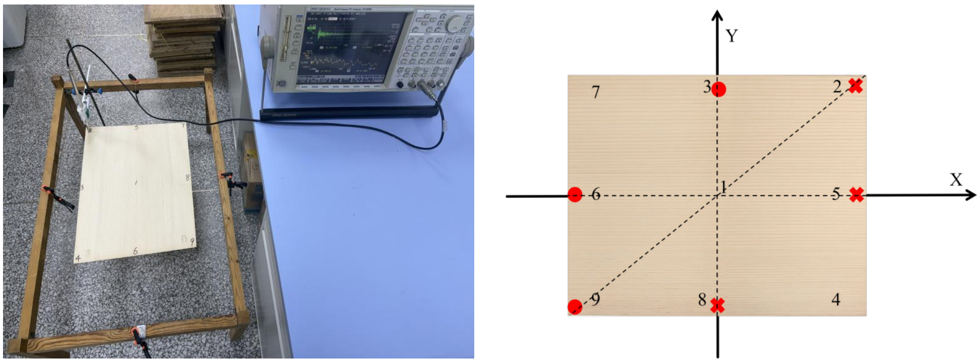

(a) **(b)**

Figure 3. Cross-intersection suspension method determination system: **(a)** Actual measurement system diagram; **(b)** diagram of incentive points distribution.

2.2.2. The principle of thickness normalization

Due to the limitations of the processing technology, the thicknesses of the specimens with different numbers of spliced panels vary: the thickness of the double-spliced resonance panel is approximately 3.8 mm, that of the triple-spliced resonance panel is about 2.9 mm, and that of the quadruple-spliced resonance panel is approximately 2.3 mm. To eliminate the influence of thickness differences on the acoustic vibration response, the time-domain signals of each specimen need to be normalized to the same reference thickness. According to the thin-plate vibration theory [27, 28], thickness changes will simultaneously alter the natural frequency (Elejabarrieta et al. used modal analysis techniques to study the vibration behavior of guitar resonance panels at various stages of construction, finding that the thickness distribution of the panel significantly affects the natural frequencies and mode shape characteristics of low-frequency modes; thinning the resonance panel will cause all modal frequencies to decrease [29]), initial amplitude, and decay rate of the resonance panel. Therefore, the normalization should be adjusted from three aspects: the time axis, amplitude, and decay.

To achieve thickness normalization, the maximum thickness among all specimens (the thickness of the double-spliced resonance panel) is taken as the reference thickness, h_{ref}. The signals of specimens with an actual thickness of h are corrected to the equivalent signals at the reference thickness. The normalization process includes the following three steps.

(1) Timeline zooming

According to the proportional relationship between frequency and thickness, the reference frequency f_{ref} at the reference thickness and the actual frequency f at the actual thickness satisfy:

$$f_{ref} = f\frac{h_{ref}}{h} \tag{14}$$

Since frequency is inversely proportional to time, the time axis of the time-domain signal should be scaled. Let the actual time axis be *t*, and the normalized time axis be t_{norm}, then there is:

$$t_{norm} = t\frac{h}{h_{ref}} \tag{15}$$

(2) Amplitude scaling

The initial peak amplitude is inversely proportional to the thickness, so the normalized amplitude is:

$$A_{ref} = A\frac{h}{h_{ref}} \tag{16}$$

(3) Attenuation compensation

The attenuation coefficient is directly proportional to the thickness. The attenuation coefficient at the actual thickness and that at the reference thickness satisfy:

$$\delta_{ref} = \delta\frac{h_{ref}}{h} \tag{17}$$

2.2.3. Calculation of time-domain characteristic parameters

In recent years, methods for analyzing sound signals have emerged in abundance [30]. MATLAB has extensive applications in the field of signal processing, especially excelling in the analysis of vibration signals . Its principle for calculating time-domain characteristic values is based on the classic mathematical definitions and statistical methods in signal processing. By analyzing the input time series signal, it extracts the main characteristic values of the vibration signal. These characteristic values reflect important information such as the energy distribution, waveform shape, and amplitude variation of the signal, providing reliable data support for the timbre analysis of vibration signals. Therefore, the vibration response data obtained through FFT will be imported into MATLAB to calculate basic time-domain characteristic parameters such as the root mean square.

Root mean square (x_{RMS}) can reflect the variation of signal strength and is used to characterize the overall intensity of the signal:

$$x_{RMS} = \sqrt{\frac{1}{N}\sum\nolimits_{i=1}^{N}(x_i)^2} \tag{18}$$

Peak-to-peak value (P_{pp}) represents the difference between the peak and the trough in a vibration signal, indicating the amplitude of the vibration signal:

$$P_{pp} = max(x_i) - min(x_i) \tag{19}$$

Kurtosis (K) is typically used to detect impulse components in vibration signals, indicating the smoothness of the waveform and describing the distribution of variables:

$$\mathrm{K} = \sqrt{\frac{1}{N}\sum\nolimits_{i=1}^{N}(x_i)^2} \tag{20}$$

2.2.4. Calculation of frequency-domain characteristic parameters

The spectral centroid (SC) reflects the "center of gravity" position of the spectral energy and is often used to measure the brightness of timbre:

$$\mathrm{SC} = \frac{\sum_{i=1}^{N} f_i x_i}{\sum_{i=1}^{N} x_i} \tag{21}$$

Spectral flatness (F) measures the "flatness" of a spectrum in the frequency domain and is the ratio of the geometric mean to the arithmetic mean:

$$\mathrm{F} = \frac{\left(\prod_{i=1}^{N} x_i\right)^{\frac{1}{N}}}{\frac{1}{N}\sum_{i=1}^{N} x_i} \tag{22}$$

Spectral kurtosis (SK) describes the "sharpness" of the spectral distribution, reflecting whether the energy is concentrated on a few frequency peaks:

$$\mathrm{SK} = \frac{\frac{1}{N}\sum_{i=1}^{N}(x_i-\mu)^4}{\left(\frac{1}{N}\sum_{i=1}^{N}(x_i-\mu)^2\right)^2} \tag{23}$$

Spectral energy (E) and frequency band energy distribution:

$$\mathrm{E} = \sum\nolimits_{i=1}^{N}(x_i)^2 \tag{24}$$

The frequency band energy distribution is to divide the entire frequency range into several consecutive sub-bands and calculate the proportion of the energy of each sub-band to the total energy.

2.2.5. Acoustic vibration characteristic evaluation parameters

The specific dynamic elastic modulus (E_{SP}) is an important indicator of the acoustic vibration performance of wood. The specific dynamic elastic modulus is the ratio of the dynamic elastic modulus of the material to its density, and when characterizing wood used for musical instruments, it can represent the average dynamic elastic modulus of the cell walls in the longitudinal direction of the wood.

$$E_{SP} = \frac{E}{\rho} \tag{25}$$

In the formula, E_{SP} represents the specific dynamic elastic modulus of the specimen, measured in km^2/s^2; E is the dynamic elastic modulus of the specimen, in GPa; and ρ is the density, in g/cm^3.

Acoustic radiation quality constant:

$$R = \sqrt{\frac{E}{\rho^3}} \tag{26}$$

In the formula, R is the acoustic radiation quality constant, $m^3/Pa \cdot s^3$; E is the dynamic elastic modulus of the specimen, GPa; ρ is the density, g/cm^3.

The speed of sound propagation (v) is one of the commonly used acoustic vibration characteristic indicators. For plate-shaped specimens, during the longitudinal wave propagation process, a certain degree of transverse propagation will occur. To avoid the influence of transverse propagation, Poisson's ratio needs to be added to the speed calculation formula to make the final obtained longitudinal wave propagation speed more accurate.

$$v = \sqrt{\frac{E}{\rho(1 - \mu_x \ \mu_y)}} \tag{27}$$

In the formula, v represents the speed of sound propagation; E is the dynamic elastic modulus of the specimen, in GPa; ρ is the density, in g/cm^3; μ_x and μ_y are the Poisson's ratios of the specimen in the x and y directions, respectively. $(1 - \mu_x \ \mu_y)$ is usually taken as 0.99.

Acoustic impedance, also known as characteristic impedance, reflects the damping characteristics of particles at a certain position in the medium caused by mechanical disturbances.

$$W = \sqrt{E\rho} \tag{28}$$

In the formula, W represents acoustic impedance; E is the dynamic elastic modulus of the specimen, in GPa; ρ is the density, in g/cm^3.

3. Results and discussion

3.1. Time-domain feature analysis

The root mean square value reflects the average energy level of the signal and is directly related to the vibration intensity of the resonance panel; the peak-to-peak value characterizes the maximum dynamic range of the vibration amplitude, indicating the initial conversion efficiency of the striking energy; kurtosis is highly sensitive to sudden spikes in the waveform, with a high kurtosis value indicating the presence of significant transient impacts in the signal; skewness is used to describe the asymmetry of the waveform and can be used to determine whether the distribution of positive and negative amplitudes during the attenuation process is balanced. When the guitar resonance panel is in actual operation, the vibration situation is rather complex, with different frequencies and modes being prominent at different excitation points [28]. It is necessary to analyze the time-domain characteristics of the vibration signals at different points, and this can also better explore the influence of the glue joint layout on the time-domain characteristics of the resonance panel vibration signals.

As shown in **Figure 4**, after thickness normalization, the RMS and peak-to-peak values of the double-spliced, triple-spliced, and quadruple-spliced resonance panels at three points exhibit a consistent pattern: the double-spliced panel has the largest values, followed by the quadruple-spliced panel, and the triple-spliced panel has the smallest values. This indicates that the double-spliced panel has the highest vibration energy level, the quadruple-spliced panel is in the middle, and the triple-spliced panel has the lowest. This is primarily because:

1. The symmetry of adhesive joint layout significantly affects modal coupling efficiency. The magnitude of vibrational energy depends on the product of mode shape amplitudes between the excitation point and the response point across various modes (i.e., modal coupling strength), rather than solely on the number of adhesive joints. The double-spliced resonance panel contains only one central adhesive joint, resulting in a highly symmetric structure with typical modal shapes that achieve the strongest modal coupling with the excitation point, thus generating the highest vibration energy. In the quadruple-spliced resonance panel, three adhesive joints are symmetrically distributed. Although the number of joints increases, symmetry ensures that bending wave energy is uniformly scattered across the panel, maintaining relatively good symmetry in each mode. As a result, effective modal coupling between the excitation and response points remains largely unaffected, allowing vibration energy to remain at a high level. In contrast, the triple-spliced resonance panel features an asymmetric adhesive joint configuration that disrupts both geometric and stiffness symmetry of the panel. This causes distortion in the modal shapes, potentially shifting the originally symmetric antinodes, thereby reducing the modal coupling efficiency between the excitation and response points and leading to the lowest vibration energy.
2. Localized energy dissipation increases due to the asymmetry of adhesive joints. As discontinuous interfaces affecting stiffness and damping, the arrangement of adhesive joints directly influences the propagation path and energy dissipation of bending waves. In the quadruple-spliced resonance panel, the symmetric adhesive joints cause multiple reflections and scatterings of bending waves within the panel; however, the symmetry maintains phase coherence during wave propagation, keeping energy dissipation relatively controlled. In the triple-spliced resonance panel, the asymmetric joints break this phase coherence, causing strong reflections, transmissions, and mode conversions at the joints, which excite more higher-order modal components. Higher-order modes typically exhibit greater damping ratios and more complex node distributions, leading to rapid energy dissipation during transmission. Consequently, the overall vibration energy in the triple-spliced resonance panel is lower than that in the quadruple-spliced resonance panel.

The variation patterns of the root mean square and peak-to-peak values measured at different positions on each resonance panel showed differences: both the double-spliced resonance panel and the quadruple-spliced resonance panel followed the pattern of (9, 2) > (6, 5) > (3, 8); however, the triple-spliced resonance panel exhibited an abnormal phenomenon, with the (6, 5) position having the largest root mean square and peak-to-peak values, followed by the (9, 2) position, and the (3, 8) position having the smallest. This is because the double-spliced panel has a symmetrical structure, with the (9, 2) position located at the (1, 1) mode antinode, having the strongest modal coupling and thus the largest vibration response; the (6, 5) position is second, and the (3, 8) position is close to the nodal line, having the weakest modal coupling. The quadruple-spliced panel has the most glue seams, but they are symmetrically distributed, with uniform energy distribution and small mode shape distortion, so the variation pattern is consistent with that of the double-spliced panel. The triple-spliced panel, due to the asymmetry of the glue seams, disrupts the geometric and stiffness symmetry of the panel, causing the modal shape to distort: the original (1, 1) mode antinode shifts from the (9, 2) position to the (6, 5) position, enhancing the modal coupling at the (6, 5) position, and since the damping at this position is relatively low, the root mean square and peak-to-peak values abnormally exceed those at the (9, 2) position. This result reveals the influence of the symmetry of the glue seam layout on the vibration energy transfer path, and the asymmetric structure of the triple-spliced panel can alter the traditional antinode distribution, concentrating the vibration energy at the (6, 5) position.

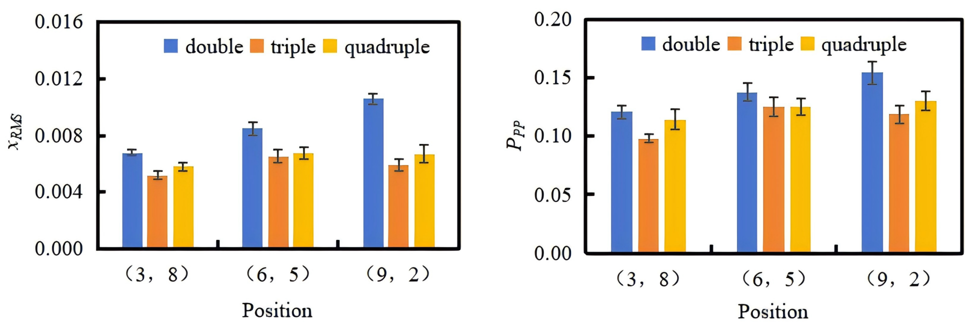

(a) **(b)**

Figure 4. **(a)** The root mean square value of the time-domain signal amplitude of the guitar's resonance panel under excitation at different points; **(b)** The peak-to-peak value of the time-domain signal amplitude of the guitar's resonance panel under excitation at different points.

Kurtosis, as a measure of the impact of the waveform, is highly sensitive to the concentration degree of modal coupling, the contribution of higher-order modes, and local damping. As shown in **Figure 5**, because the double-spliced resonance panel structure is symmetrical, the modal shape is typical, and the (9, 2) point is located at the antinode of the (1, 1) mode, which has a strong coupling with this mode, resulting in the lowest kurtosis; the (3, 8) point is close to the nodal line, with multiple modal couplings, and the waveform contains transient spikes of higher-order modes, increasing the impact, and thus has the highest kurtosis. The quadruple-spliced resonance panel has many glue seams, but they are symmetrically distributed, with energy being uniformly scattered, and the modal coupling characteristics at each point tend to be consistent, with similar waveform shapes, so the (3, 8) point has the highest kurtosis, and the (6,

5) point has the lowest. The triple-spliced resonance panel, due to the asymmetry of the glue seams, disrupts the geometric and stiffness symmetry of the panel, leading to distortion of the modal shape and changes in the modal coupling pattern. The asymmetric glue seams introduce more higher-order modal components and enhance the coupling between modes, causing numerous transient spikes in the waveform, so the kurtosis at each point is higher than that of the double-spliced and quadruple-spliced resonance panels; among them, the (3, 8) point has the most complex multi-modal coupling and the highest kurtosis, while the (6, 5) point, because the line connecting the excitation point and the response point is parallel to the splice seam, has a relatively simple modal coupling and phase superposition in this direction, resulting in the lowest kurtosis.

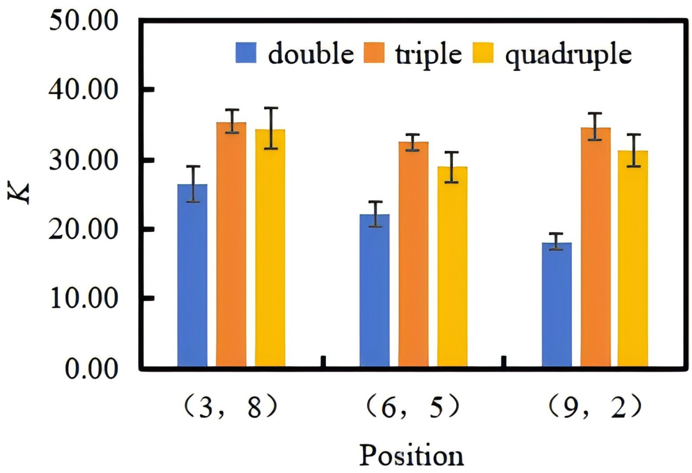

Figure 5. The kurtosis of the time-domain signal of the guitar resonance panel under excitation at different points.

3.2. Frequency domain feature analysis

The spectral characteristics reveal the distribution law of the vibration energy and the radiation properties of the resonance panel from the frequency domain perspective, and they are the important basis for evaluating the brightness, balance, and high-frequency response of the timbre. After the thickness normalization processing, the spectra of the panels with different numbers of spliced boards have been aligned under the unified thickness benchmark, and their frequency domain characteristics can be directly compared. Considering that the resonance frequencies of each order are most prominent when the excitation is at the (9, 2) position, the frequency domain features of each panel when excited at the (9, 2) position are compared in this section.

The spectral centroid is the weighted average frequency of the spectral energy, reflecting the "brightness" of the sound. A higher value indicates a richer high-frequency energy. By calculating the spectral centroid and the energy proportion of the high-frequency band (200–500 Hz) for each specimen, the influence of the number of glue joints on the high-frequency components can be quantitatively analyzed, revealing the variation pattern of the timbre brightness of multi-spliced resonance panels. As shown in **Figure 6**, from the double-spliced resonance panel to the quadruple-spliced resonance panel, both the spectral centroid and the high-frequency energy proportion show a trend of initially rising significantly and then declining. The spectral centroid and the high-frequency energy proportion are determined by the coupling characteristics of each mode between the excitation point and the response point, and are jointly affected by the layout of the glue joints and the structural symmetry. As can be seen from **Figure 7**, the double-spliced resonance panel only contains a central glue joint and is structurally symmetrical. The (9, 2) point is at the antinode of the (1, 1) mode, with strong coupling, and the energy is mainly concentrated in the low-order modes, thus the spectral centroid and the high-frequency energy proportion are relatively low. The triple-spliced resonance panel has an asymmetrical glue joint layout, which disrupts the geometric and stiffness symmetry of the panel, causing the modal shape to distort. The originally symmetrical modes split, the contribution of the mid-to-high frequency modes increases, and the coupling with the excitation point increases, resulting in the energy shifting to the mid-to-high frequency range, and the spectral centroid and the high-frequency energy proportion rise. Although the quadruple-spliced resonance panel has more glue joints, they are symmetrically distributed, and the energy is evenly scattered, with a more uniform modal distribution. Although high-order modes still exist, the symmetry causes the energy distribution to tend to be balanced across all frequency bands, avoiding excessive concentration in the mid-to-high frequency range. Therefore, the spectral centroid and the high-frequency energy proportion are slightly lower than those of the triple-spliced resonance panel. This result reveals the influence of the symmetry of the glue joint layout on the frequency domain distribution of energy: the asymmetrical structure of the triple-spliced resonance panel can enhance the mid-to-high frequency components, causing the spectral centroid to shift upward; the symmetrical multi-glue joint structure of the quadruple-spliced resonance panel evenly scatters the energy, making the spectral centroid and the high-frequency energy proportion return to a moderate level.

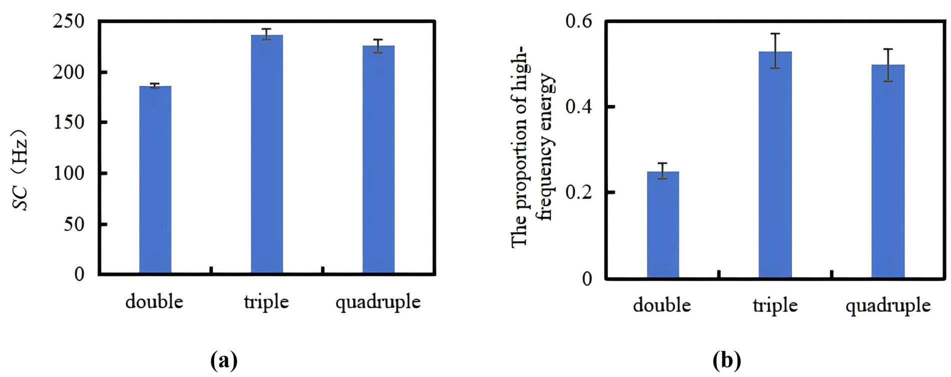

Figure 6. (a) The spectral centroid of the frequency domain signal of the guitar's resonance panel; **(b)** The proportion of high-frequency energy in the frequency domain signal of the guitar's resonance panel.

Spectral flatness describes the uniformity of the spectral line energy distribution. A flatness value close to 1 indicates that the energy is evenly distributed across all frequencies, while a value close to 0 suggests that the energy is concentrated in a few frequencies. Spectral kurtosis measures the sharpness of the spectral peak, with a high kurtosis value indicating the presence of distinct resonance peaks. Spectral flatness reflects the uniformity of energy distribution in the frequency domain, which is jointly influenced by the modal distribution density and the modal coupling strength. As shown in **Figures 7** and **8**, the double-spliced resonance panel has only one central glue joint, with a symmetrical structure and typical modal shapes. The energy is mainly concentrated in a few low-order modes (such as the (1, 1) mode), resulting in a spectrum with distinct discrete peaks, low flatness, and the highest kurtosis. The triple-spliced resonance panel, due to the asymmetry of the glue joints, disrupts the geometric and stiffness symmetry of the panel, causing modal shape distortion and modal splitting. The original modal frequencies separate, the modal distribution density increases, and the contribution of mid-to-high frequency modes enhances, leading to a more uniform energy distribution across a wider frequency band. The spectral envelope tends to be flat, and the energy disperses over a broader frequency range, resulting in a decrease in kurtosis and an increase in spectral flatness. The quadruple-spliced resonance panel, despite having multiple glue joints, has a symmetrical distribution, with energy being uniformly scattered. The modal distribution is denser and more uniform, but the symmetry leads to a more coordinated coupling between modes, which may cause some fluctuations in the spectral envelope. Therefore, the flatness is slightly lower than that of the triple-spliced panel but still higher than that of the double-spliced panel. The kurtosis slightly increases compared to the triple-spliced panel but remains lower than that of the double-spliced panel, being close to that of the triple-spliced panel. The asymmetrical structure of the triple-spliced panel flattens the spectrum through modal splitting; the symmetrical multi-glue joint structure of the quadruple-spliced panel maintains a moderate spectral flatness through uniform energy scattering.

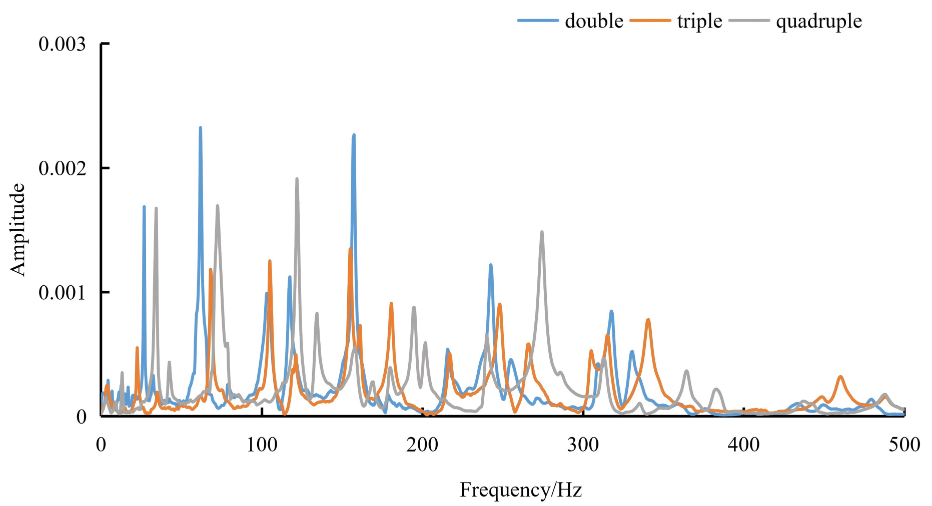

Figure 7. Spectrograms of resonance panels of different structures after thickness normalization.

It can be observed that the triple-spliced resonance panel exhibits the following characteristics:

1. A higher spectral centroid and significantly increased mid-to-high frequency energy (200–350 Hz), giving it a brighter tonal tendency;
2. The highest spectral flatness, with the most uniform energy distribution across

frequency bands, results in clean and clear sound reproduction;
3. The lowest overall vibration energy (both RMS and peak-to-peak);
4. The strongest waveform impulsiveness (higher kurtosis), indicating a relatively sensitive dynamic response.

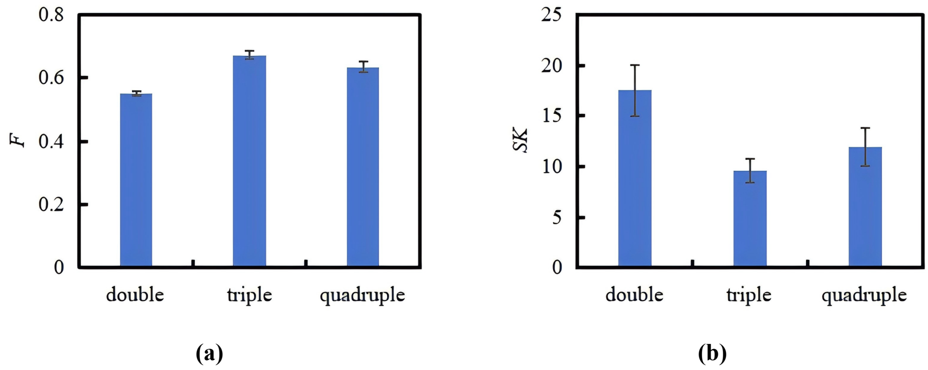

Figure 8. **(a)** The spectral flatness of frequency domain signals of guitar resonance panels with different structures; **(b)** The spectral kurtosis of frequency domain signals of guitar resonance panels with different structures.

Based on these properties, the triple-spliced resonance panel holds potential for specific performance styles. For instance, fingerstyle playing emphasizes note clarity, articulation, and balance among voices, demanding high sensitivity to sustain and dynamic nuances. The even spectral distribution and bright tone of the triple-spliced panel help highlight melodic outlines and harmonic layers, making it particularly suitable for musical genres requiring strong high-frequency overtones (such as lyrical pieces or country fingerstyle). However, its relatively low overall energy may affect volume projection, potentially placing it at a disadvantage compared to double-spliced panels in unamplified acoustic settings. Strumming techniques require panels with strong dynamic responsiveness and high-volume output. While the enhanced mid-to-high frequencies of the triple-spliced panel can produce a brighter strumming tone, its lower energy output may result in insufficient volume during intense strumming, and the highly impulsive waveform could generate excessive sharpness under extreme dynamics. Therefore, this panel type may be better suited for moderate-intensity strumming or ensemble settings where a bright tonal color is desired, rather than for extremely loud performances. It should be emphasized that the above analysis is based on theoretical deductions from objective physical parameters and has not yet been validated by subjective listening tests conducted by professional musicians. Ultimately, the acoustic quality of an instrument must be evaluated through a combination of objective measurements and subjective perception.

Traditional luthiers use tapping tuning as an empirical, subjective evaluation method, primarily involving tapping different areas of the resonance panel and listening to the resulting acoustic responses (pitch, timbre, etc.), then making fine adjustments to panel thickness distribution and bracing cuts accordingly. This approach essentially relies on subjective auditory judgment of the panel’s vibrational characteristics, whereas the FFT analysis used in this study provides an objective quantitative representation of the same physical process—the frequency spectrum of the vibration signal. Drawing upon existing research in psychoacoustics, we have established a correlation between objective spectral parameters and subjective auditory perception (**Table 3**).

Table 3. Correlation table between objective spectral parameters and subjective listening perception.

Objective parameters	Physical meaning	Subjective listening perception corresponds
Spectral Centroid	Center frequency of the spectral energy distribution	Brightness of timbre. The higher the centroid, the brighter the sound; the lower the centroid, the warmer and richer the perception.
Spectral Kurtosis	Sharpness of the spectral distribution	Sound impact/penetration. The higher the kurtosis, the stronger the transient response.
Spectral Flatness	The balance of energy across the frequency band	Sound balance/clarity. The flatter the response, the cleaner and more balanced the tone.
Bandwidth energy distribution	Energy distribution across frequency bands	Tonal warmth tendency (higher proportion of mid and high frequencies → bright, higher proportion of low frequencies → warm)

3.3. Mechanical property and acoustic vibration parameter analysis

Mechanical properties are one of the inherent characteristics of materials. For wood, mechanical properties have a significant impact on the acoustic vibration performance of wood. Therefore, it is necessary to study the mechanical properties of three types of resonance panels and their raw materials, and to determine the influence law of structural changes on their mechanical properties.

The modulus of elasticity is an important indicator for measuring the stiffness characteristics of wood, representing the ability of solid materials to resist elastic deformation. As shown in **Figure 9**, with the increase of the glue joint, from the double-spliced resonance panel to the quadruple-spliced resonance panel, the longitudinal and radial modulus of elasticity of the resonance panel show an upward trend. Compared with the raw material, the longitudinal modulus of elasticity of the three types of spliced panels increased by 1.42%, 3.65%, and 11.50%, respectively, and the radial modulus of elasticity of the three types of spliced panels increased by 5.79%, 11.50%, and 15.59%, respectively. The growth rate also shows an increasing trend.

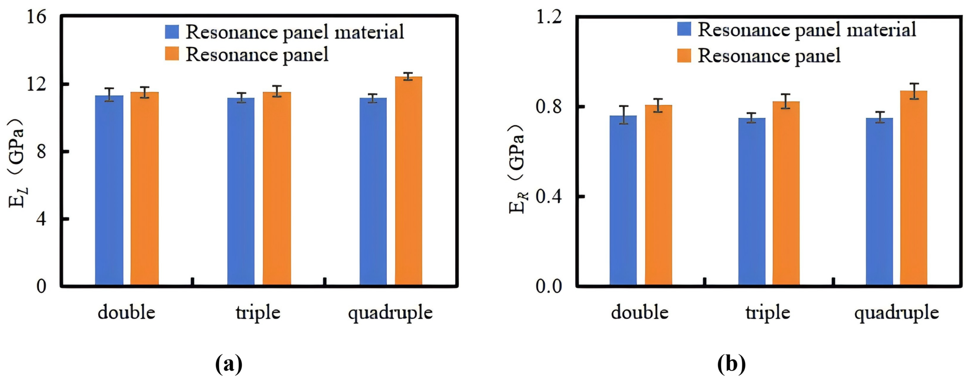

Figure 9. **(a)** The longitudinal elastic modulus of different structure resonance panels and materials of guitars; **(b)** The radial elastic modulus of different structure resonance panels and materials of guitars.

The shear modulus is one of the important mechanical performance indicators of materials, characterizing the material's ability to resist shear strain. The torsional vibration of the guitar resonance panel during vibration cannot be ignored, and it is necessary to explore the influence law of structural changes on its shear modulus. As can be seen from **Figure 10**, with the increase in the number of splicing seams, from the double-spliced resonance panel to the quadruple-spliced resonance panel, the shear modulus of the resonance panel shows an upward trend. Compared with the original material, the shear modulus of the three types of spliced panels increased by 10.03%, 17.73%, and 21.83%, respectively. This indicates that structural changes increase the shear modulus, and the influence is greater compared to the elastic modulus.

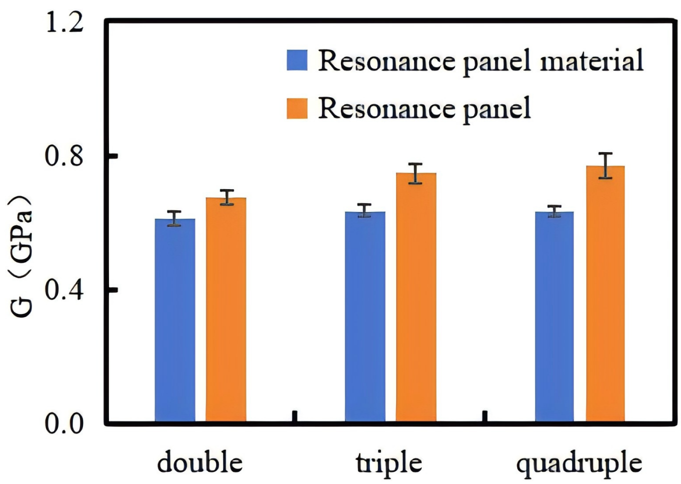

Figure 10. The shear modulus of different structure resonance panels and materials of guitars.

After the application of adhesive, the overall elastic modulus and shear modulus of the resonance panel increase compared to before the assembly. The core reason for this lies in the formation of a physical "composite reinforcement" effect and a chemical/physical "penetration strengthening" between the adhesive and the wood. This is not because the modulus of the adhesive itself is much higher than that of the wood, but mainly due to:

1. The adhesive penetrates and enhances the wood cell walls (microscopic reinforcement). When the adhesive is applied and pressed, it penetrates into the tracheid (cell) cavities and cell walls on the wood surface, forming a "wood-plastic composite" interface layer. Research shows that when resin penetrates the wood tracheid wall layer, it can significantly improve the microscopic mechanical properties of the cell walls. For example, after phenolic resin (PF) penetration, the elastic modulus of the wood tracheid wall can increase by about 7%, and the hardness can increase by about 26%. This means that the originally relatively loose wood surface is "reinforced," forming a transition layer with higher mechanical properties.
2. The adhesive layer fills the natural defects (structural reinforcement). After sawing, the surface of the log board has small ripples, cracks, or vessel pores. During the assembly, the adhesive layer fills these defects, forming a continuous stress transfer path. Although the cured adhesive layer is a polymer material, its elastic modulus (about 2.5–4.0 GPa after curing) is sufficient to bear the load. Studies show that by adding fillers to the adhesive, its elastic modulus can be increased from 2.3 GPa to 4.4 GPa, and even by enhancing with nanomaterials

(such as graphene, nano-silica), the adhesive can further improve the mechanical properties of the overall composite panel.

3. The composite effect enhances the overall stiffness (macroscopic reinforcement). From a macroscopic mechanical perspective, the assembled resonance panel can be regarded as a composite material composed of "wood-adhesive-wood." The adhesive effectively combines the wood on both sides into a whole, ensuring that they can deform in coordination when subjected to force. This significantly improves the panel's ability to resist bending deformation (reflected in the increase of elastic modulus) and shear slippage (reflected in the increase of shear modulus). It can also be observed that the modulus of elasticity increase in triple-spliced resonance panels is smaller than that in quadruple-spliced resonance panels. This is primarily because the reinforcing effect of adhesive joints on the panel's elastic modulus does not follow a simple linear superposition, and is mainly influenced by the following two factors:

    (1) The position distribution of adhesive joints within the cross-section. Double-spliced resonance panels have only one central adhesive joint, resulting in limited improvement in overall stiffness. In triple-spliced resonance panels, the two adhesive joints divide the panel into three sections—one wider section on one side and two narrower sections on the other—with the joints located near the edges, thus contributing relatively less to bending stiffness. In contrast, the three adhesive joints in quadruple-spliced resonance panels evenly divide the panel width into four sections, with uniformly distributed joints, leading to a more significant enhancement in overall stiffness. In other words, the effective cross-sectional contribution of adhesive joints depends not only on their number but also on their distance from the neutral axis and their relative positioning.

    (2) The synergistic strengthening effect of multiple adhesive joints: when several adhesive joints are arranged parallel to each other, the wood matrix between them is divided into multiple narrow strips. As the width-to-thickness ratio of each strip decreases, local buckling or shear deformation becomes constrained, thereby generating higher overall stiffness than would result from simply summing the effects of individual joints. This synergistic effect is particularly pronounced in quadruple-spliced resonance panels.

Given that the longitudinal elastic modulus E_L of the sample is much greater than the radial elastic modulus E_R (the former is usually several times the size of the latter), the acoustic vibration performance of the sample mainly depends on the elastic modulus E_L. Therefore, only the acoustic vibration characteristic indicators in the longitudinal direction are calculated. The acoustic vibration indicators measured under each suspension condition are averaged, and the acoustic vibration characteristic parameters of the three types of resonance panels and materials are calculated and analyzed.

As shown in **Figure 11**, the specific dynamic elastic modulus E_{SP} can represent the average dynamic elastic modulus of the cell walls in the longitudinal direction of wood. The higher its value, the better the acoustic vibration performance of the material. Among the three types of guitar resonance panels, the quadruple-spliced resonance panel has the largest specific dynamic elastic modulus, which is 24.90 km^2/s^2; followed by the triple-spliced resonance panel with a value of 24.73 km^2/s^2; the smallest is the double-spliced resonance panel, with a value of 24.32 km^2/s^2. From the double-spliced resonance panel to the quadruple-spliced resonance panel, the specific dynamic elastic modulus shows an upward trend. Compared with the original material, the growth rate of the specific dynamic elastic modulus before and after splicing also shows an upward trend. This is mainly because the adhesive used at the splicing joints increases the overall elastic modulus of the panel, further enhancing the specific dynamic elastic modulus. The acoustic radiation quality constant *R* is a parameter used to evaluate the quality of sound radiation of wood. Among the three types of guitar resonance panels, the double-spliced resonance panel has the largest acoustic radiation quality constant, which is 10.29 $m^3/Pa{\cdot}s^3$; followed by the triple-spliced resonance panel with a value of 10.16 $m^3/Pa{\cdot}s^3$; the quadruple-spliced resonance panel has the smallest acoustic radiation quality constant, which is 10.02 $m^3/Pa{\cdot}s^3$. It can be seen that as the number of glue joints increases, from the double-spliced resonance panel to the quadruple-spliced resonance panel, the acoustic radiation quality constant shows a downward trend. This may be because the presence of the glue layer at the splicing joints affects the propagation of sound, causing it to decrease. The acoustic radiation quality constant of the quadruple-spliced resonance panel decreased by approximately 2.6% compared to that of the double-spliced resonance panel (from 10.29 to 10.02 $m^3/(Pa{\cdot}s^3)$), while the triple-spliced resonance panel showed a decrease of about 1.3%. From an engineering perspective, this change in magnitude typically has a minor practical acoustic impact and may be difficult to perceive during actual playing. In this study, perceived volume is more influenced by the proportion of mid- to high-frequency energy (the frequency range most sensitive to human hearing). The quadruple-spliced resonance panel exhibits higher mid- to high-frequency energy than the double-spliced one, partially compensating for any potential volume loss due to the reduced *R* value. The final volume of a finished guitar depends not only on the *R* value of the soundboard but also on multiple factors, including the back plate, side plates, bracing layout, and body cavity coupling. Therefore, a slight reduction in *R* value may be masked or compensated by other factors in actual instruments. The acoustic impedance *W*, also known as the characteristic impedance, refers to the resistance of the propagation medium to the propagation of sound. Among the three types of guitar resonance panels, the quadruple-spliced resonance panel has the largest acoustic impedance, which is 2.50 MPa·s/m; followed by the triple-spliced resonance panel with a value of 2.45 MPa·s/m; the smallest is the double-spliced resonance panel, with a value of 2.37 MPa·s/m. From the double-spliced resonance panel to the quadruple-spliced resonance panel, the acoustic impedance shows an upward trend. Compared with the original material, the growth rate of the acoustic impedance of the three types of panels after splicing also shows an upward trend. This is mainly because the presence of the glue layer increases the resistance to sound reflection inside the panel. The more glue layers there are, the greater the resistance to sound reflection. The sound propagation speed v is one of the commonly used acoustic vibration characteristic indicators. From the double-spliced resonance panel to the quadruple-spliced resonance panel, the sound propagation speed gradually increases, but the growth rate is very small. The sound propagation speed of the three types of panels is all greater than that of their original materials. This is mainly because, with the increase of glue joints, the mechanical properties of the panels, from the original material to the panels, and from the double-spliced resonance panel to the quadruple-spliced resonance panel, are improved, which is beneficial to the propagation of sound.

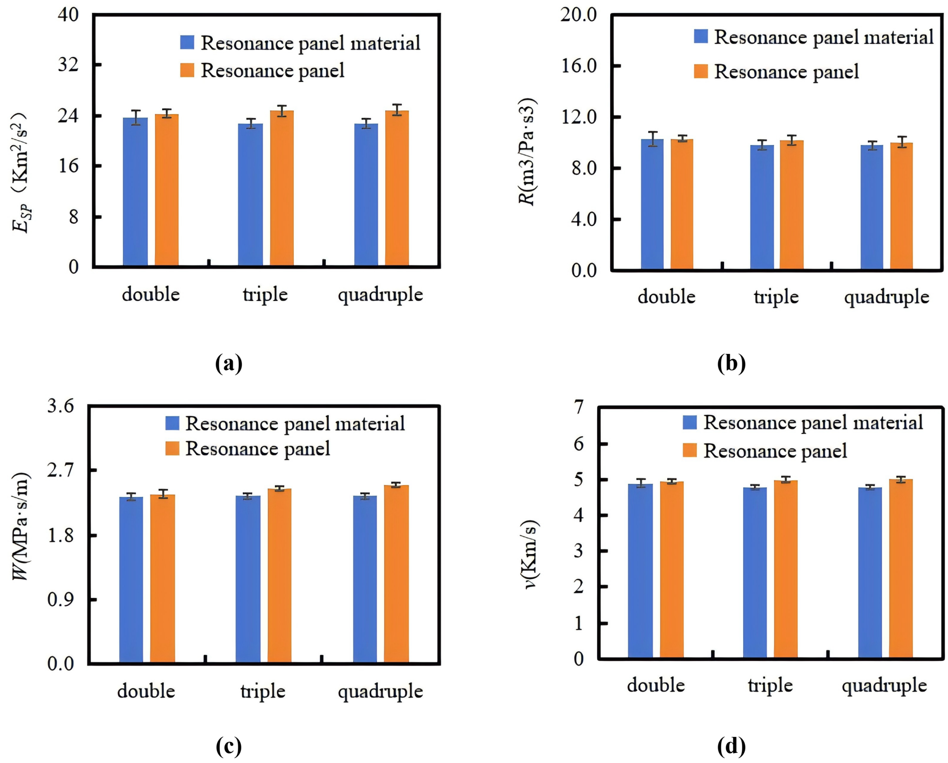

Figure 11. **(a)** The specific dynamic elastic modulus of different structural resonance panels and materials; **(b)** The acoustic radiation quality constant of different structural resonance panels and materials; **(c)** The acoustic impedance of different structural resonance panels and materials; **(d)** The sound propagation speeds of different structural resonance panels and materials.

3.4. Cost analysis

Currently, guitar manufacturers commonly use semi-automated or fully automated panel splicing equipment (including processes such as gluing, high-precision joining, and sanding, and curing). This study conducted a cost analysis of different splicing configurations under identical production capacity. The results show that the overall cost of quadruple-spliced resonance panels is approximately 27% lower than that of double-spliced resonance panels. Although multi-spliced panels involve additional processing steps such as cutting, edge finishing, joining, and gluing, their cost advantage mainly stems from two factors: first, narrow-width boards are significantly cheaper to purchase than wide-width boards, and the substantial reduction in raw material costs more than offsets the extra processing expenses;

second, the semi-automation/automation of manufacturing effectively controls labor costs, resulting in a much smaller increase in per-unit labor cost compared to the savings in material costs. Therefore, the economic feasibility of multi-spliced panels is well established. In summary, adopting quadruple-spliced resonance panels not only alleviates the pressure caused by the shortage of high-quality large-format spruce materials but also enables optimization of product costs while maintaining acceptable acoustic performance.

4. Discussion

This study reveals a seemingly contradictory phenomenon: the triple-spliced resonance panel exhibits the lowest overall vibration energy yet produces the brightest tone and the most uniform frequency spectrum. However, this is not physically contradictory and can be reasonably explained from a psychoacoustic perspective. The energy of the triple-spliced resonance panel is concentrated in the mid-to-high frequency range of 200–350 Hz, with a relatively even distribution across bands; in contrast, the double-spliced resonance panel has energy highly concentrated in the low-frequency band of 50–200 Hz. When the spectral centroid (indicating the center of energy concentration) shifts toward higher frequencies, listeners perceive the tone as brighter. Considering the frequency-dependent sensitivity of human hearing, the ear is most sensitive to the 2–5 kHz range and less responsive to low-frequency components. Although the double-spliced panel has higher low-frequency energy, its perceived efficiency by the human ear is lower. Conversely, although the absolute energy levels in the mid-to-high frequency range of the triple-spliced panel are not particularly high, the ear's perception efficiency in this range is greater, resulting in a more pronounced sense of brightness. The triple-spliced panel also shows the highest spectral flatness, indicating the most uniform energy distribution across frequency bands—a balanced quality often described by performers as clean, clear, or expressive. Furthermore, the triple-spliced panel displays the strongest waveform impulsiveness (highest kurtosis and significant peak factor), which may produce a more penetrating sound during fast playing or strong articulation. In contrast, the double-spliced panel's lower kurtosis and nearly sinusoidal waveform tend to deliver a smoother and warmer auditory sensation. Therefore, there is no simple positive correlation between vibration energy and tonal brightness.

5. Conclusion

In this study, the vibration signals of three types of spruce guitar resonance panels were measured under free boundary conditions. The time-domain characteristics, frequency-domain characteristics, mechanical properties, and acoustic vibration parameters were analyzed and compared, and the following conclusions were drawn:

The consistent patterns shown in the root mean square values (indicating the overall intensity of the vibration signal) and peak-to-peak values (indicating the amplitude of the vibration signal) of the three types of panels suggest that the double-spliced resonance panel has the greatest vibration energy, followed by the quadruple-spliced resonance panel, and the triple-spliced resonance panel has the least. This is because the asymmetrical glue joint layout of the triple-spliced resonance panel intensifies energy dissipation, while the symmetrical multi-glue joint layout of the quadruple-spliced resonance panel makes the energy distribution more uniform. This indicates that structural changes can alter the magnitude of the vibration energy of the panels.

Spectral centroid and high-frequency energy distribution characterize the brightness and richness of high-frequency energy of timbre, while spectral flatness and kurtosis represent the uniformity of energy distribution. From double-spliced resonance panels to quadruple-spliced resonance panels, the spectral centroid and high-frequency energy distribution, as well as spectral flatness, show a trend of first rising and then falling, while spectral kurtosis shows the opposite trend. This indicates that the triple-spliced resonance panel has the greatest timbre brightness and the most uniform spectral energy distribution, followed by the quadruple-spliced resonance panel, and the double-spliced resonance panel has the least timbre brightness and the most uneven spectral energy distribution. This is because the asymmetric glue joint layout of the triple-spliced resonance panel can enhance the mid- and high-frequency components, while the symmetrical multi-glue joint layout of the quadruple-spliced resonance panel makes the energy distribution more balanced through uniform scattering. It demonstrates that structural changes can alter the distribution of vibration energy in the resonance panel and thereby regulate the brightness of the timbre. Enterprises can obtain the desired sound brightness by changing the structure of the resonance panel according to their needs.

From the double-spliced resonance panel to the quadruple-spliced resonance panel, the elastic modulus and shear modulus of the panels show an increasing trend. Compared with the original material, the longitudinal elastic modulus of the three types of spliced panels increased by 1.42%, 3.65%, and 11.50%, respectively; the radial elastic modulus increased by 5.79%, 11.50%, and 15.59%, respectively; and the shear elastic modulus increased by 10.03%, 17.73%, and 21.83%, respectively. The specific dynamic elastic modulus shows an upward trend, while the acoustic radiation quality constant shows a downward trend. The acoustic impedance gradually increases, and the increase in the speed of sound propagation is very small. This is because the adhesive and wood form a physical "composite reinforcement" effect and a chemical/physical "penetration strengthening" effect, effectively enhancing the mechanical properties of the panels. However, the presence of the adhesive layer also increases energy dissipation. Compared with the double-spliced panel, the triple-spliced panel and quadruple-spliced panel have better mechanical properties and acoustic vibration performance close to the former. This indicates that structural changes can improve the mechanical properties of the panels without compromising their acoustic vibration performance. Double-spliced resonance panels are suitable for high-end instruments with extremely demanding acoustic performance requirements, such as professional-grade guitars; whereas multi-spliced panels—especially quadruple-spliced resonance panels—can serve as a viable alternative for mid-to-high-end or entry-level instruments. Multi-spliced panels effectively utilize narrow-width lumber, thereby improving the overall utilization of premium spruce resources. For manufacturers focused on environmental sustainability and cost control, a 2.6% reduction in acoustic radiation quality constant is an acceptable trade-off, demonstrating the potential of multi-spliced panels to replace double-spliced panels. which is of great significance for conserving forest resources and guiding enterprise production.

The prospects and limitations of this study are as follows:

1. The sample size in this study is relatively small; future research could expand the sample size and conduct statistical analyses.
2. The final assessment of an instrument's acoustic quality should be verified through subjective listening tests by professional musicians. This study currently focuses on objective parameter measurement and comparison. Future research could proceed in the following directions:

   (1) Spectral characterization of tapping sounds—using the same measurement system to capture acoustic signals when traditional luthiers tap resonance panels, extracting spectral features such as centroid, kurtosis, and flatness, and conducting correlation analysis between these parameters and the luthiers' qualitative evaluations (e.g., brightness, balance, sustain), thereby establishing a mapping database linking auditory descriptions to objective spectral parameters;

   (2) Double-blind listening tests—inviting experienced luthiers and performers to blindly evaluate three-piece, four-piece, and double-spliced resonance panels, subjectively rating them on dimensions such as brightness, balance, dynamic response, and sustain, and analyzing correlations and performing regression modeling with objective parameters obtained via FFT;

   (3) Development of an evaluation model—based on multiple sets of subjective-objective comparative data, exploring the establishment of a quantifiable and reproducible model for assessing the acoustic quality of guitar resonance panels, providing a scientific tool for the digital preservation of traditional luthiery techniques.

3. The conclusions drawn from this study under rectangular bare-plate conditions cannot be directly extrapolated to complete guitars. Subsequent work will proceed in two stages: Stage one (completed): using rectangular bare plates as models, investigating the influence patterns of glue-line number and thickness distribution on panel acoustic vibration performance, and establishing a foundational database. Stage two (planned):

   (1) Gradually adding fan braces onto the rectangular bare plate, analyzing the coupled effects among braces, spliced panels, and thickness;

   (2) Assembling with side and back panels to form a closed soundbox, studying the impact of cavity air modes on the vibration characteristics of multi-spliced panels;

   (3) Establishing a full-scale guitar finite element model using COMSOL,

validating it experimentally, and conducting parametric expansion analysis to predict the acoustic performance of different spliced-panel configurations in complete guitars;

(4) Ultimately, collaborating with musical instrument manufacturers to produce finished guitars for subjective listening tests, verifying the practical application value of this research.

4. Minor differences caused by natural wood variation cannot be entirely ruled out. Due to experimental limitations, density gradient measurements or CT scans to quantify microstructural differences were not performed on all specimens. Although the influence of natural wood variability has been minimized as much as possible, future studies plan to employ methods such as thermal modification or chemical treatments to further homogenize material properties.
5. Experimental validation of the effectiveness of thickness normalization was not conducted. Future research could prepare independent test samples with reference thickness, directly comparing measured signals with normalized signals to further verify the accuracy of this method.

Author contributions: Conceptualization, GW and ZL; methodology, GW, ZL; software, GW, JC and LZ; validation, GW, SW and YB; formal analysis, GW and HC; investigation, GW and LH; resources, GW; data curation, GW and YZ; writing—original draft preparation, GW; writing—review and editing, GW, LZ; visualization, GW; supervision, ZL; project administration, ZL; funding acquisition, ZL. All authors have read and agreed to the published version of the manuscript.

Funding: This research was funded by the National Natural Science Foundation of China, grant number 32271781.

Institutional review board statement: Not applicable.

Informed consent statement: Not applicable.

Data availability statement: All data supporting the findings of this study are available within the article.

Conflict of interest: The authors declare no conflict of interest.

AI use statement: During the preparation of this manuscript, the authors used AI tools solely for language refinement. No AI tools were used for data analysis, interpretation, or generation of scientific content. All outputs were critically reviewed and edited by the authors. The authors take full responsibility for the integrity and accuracy of the work.

References

1. Roldan-Cardona M, Chacón-Castro M, Jadán-Guerrero J, et al. Music Education with Artificial Intelligence for Inclusive and Sustainable Early Childhood Learning. Emerging Science Journal. 2025; 9: 201–218. doi: 10.28991/ESJ-2025-SIED1-012
2. Fletcher NH, Rossing TD. Guitars and Lutes. In: The Physics of Musical Instruments. Springer; 1991. pp. 207–234.

doi: 10.1007/978-1-4612-2980-3_9

3. Liang Y, He L, Zhang L, et al. Effects of Oil Heat Treatment on the Acoustic Vibration Properties of Bamboo. Forest Engineering. 2024; 40(3): 115–124. Available online: https://slgc.nefu.edu.cn/EN/10.3969/j.issn.1006-8023.2024.03.011 (in Chinese)
4. Plath N, Linke S, Mores R. On the angle-dependent vibrational behavior of fiber composite plates and its implications for musical instrument making. The Journal of the Acoustical Society of America. 2022; 151(3): 1956–1970. doi: 10.1121/10.0009799
5. Hao Qian. Research on the Preparation and Acoustic Vibration Properties of Birch Veneer-Metal Composite Materials [Master's Thesis]. Northeast Forestry University; 2023. Available online: https://d.wanfangdata.com.cn/thesis/ChhUaGVzaXNOZXdTMjAyNDA5MjAxNTE3MjUSCFk0MTcxMjc0Gghpb2tseHZsdw%3D%3D (in Chinese)
6. Liu Z, Li X, Yu Y, et al. Effects of wood flour and compatibilizer contents on the acoustic vibration performance of wood-plastic composites. Forest Engineering. 2022; 38(5): 62–67. Available online: https://slgc.nefu.edu.cn/EN/Y2022/V38/I5/62 (in Chinese)
7. Li J. The physical properties of wood. In: Wood Science, 3rd ed. Science Press; 2021. pp. 209–219. (in Chinese)
8. Wegst UGK. Wood for sound. American Journal of Botany. 2006; 93(10): 1439–1448. doi: 10.3732/ajb.93.10.1439
9. Damodaran A, Mansour H, Lessard L, et al. Application of composite materials to the chenda, an Indian percussion instrument. Applied Acoustics. 2015; 88: 1–5. doi: 10.1016/j.apacoust.2014.07.013
10. Fang Yi. Resonance panel. In: The Making and Appreciation of Classical Guitars. Shanghai Education Publishing House; 2010. pp. 148–154. (in Chinese)
11. Tao X, Han J, Xu W, et al. The influence of texture angle of spruce wood on the acoustic vibration performance of piano resonance panels. China Wood Industry. 2019; 33(4): 14–17. (in Chinese)
12. Manzo G, Tippner J, Zatloukal P. Relationships between the Macrostructure Features and Acoustic Parameters of Resonance Spruce for Piano Soundboards. Applied Sciences. 2021; 11(4): 1749. doi: 10.3390/app11041749
13. Gao S, Tao X, Wang X, et al. Theoretical modeling of the effects of temperature and moisture content on the acoustic velocity of Pinus resinosa wood. Journal of Forestry Research. 2018; 29(2): 541–548. doi: 10.1007/s11676-017-0440-5
14. Richardson BE. The acoustical development of the guitar. Catgut Acoustical Society Journal. 1994; 2(5): 1–10. Available online: https://www.cglib.org/wp-content/uploads/cglib.org/Musicology/The%20acoustical%20development%20of%20the%20guitar.pdf
15. Stanciu MD, Dinulică F, Bucur V, et al. Changing the vibrational behavior of the wooden thin arched plates—The maestro violins experimental study case. Thin-Walled Structures. 2022; 174: 109042. doi: 10.1016/j.tws.2022.109042
16. Viala R, Placet V, Foltête E, et al. Model based ranking of the influence of geometry and materials on the dynamical behavior of the violin highlights predominance of geometrical choices. Scientific Reports. 2024; 14(1): 29589. doi: 10.1038/s41598-024-79497-7
17. Stanciu MD, Rosca IC, Mihălcică M, et al. Dynamic response of wooden plates in different stages of guitar manufacturing. European Journal of Wood and Wood Products. 2022; 80(4): 997–1013. doi: 10.1007/s00107-022-01817-3
18. Torres JA. On Caldersmith's Measurements of Free Plates and Assembled Violins. Acoustics Australia. 2023; 51(2): 293–296. doi: 10.1007/s40857-023-00296-7
19. Lercari M, Gonzalez S, Espinoza C, et al. Using Mechanical Metamaterials in Guitar Top Plates: A Numerical Study. Applied Sciences. 2022; 12(17): 8619. doi: 10.3390/app12178619
20. Longo G, Gonzalez S, Dalisay JDE, et al. Influence of thickness profile and bracing pattern in the radiation patterns of archtop guitars. The Journal of the Acoustical Society of America. 2025; 157(2): 1141–1150. doi: 10.1121/10.0035805
21. Quintavalla M, Santini M, Nicoletti G. Survey and evaluation of classical guitar soundboard design methods with finite element analysis. The Journal of the Acoustical Society of America. 2025; 157(2): 1072–1083. doi: 10.1121/10.0035798
22. Kusumaningtyas I, Sanjaya TR, Andwir R. Vibration simulation of guitar top plates from spruce and petung bamboo at subsequent production stages. In: Proceedings of the 3rd International Conference on Mechanical Engineering (ICOME 2017); 5–6 October 2017; Surabaya, Indonesia. p. 030014. doi: 10.1063/1.5046249
23. Sobue N, Katoh A. Simultaneous Determination of Orthotropic Elastic Constants of Standard Full-Size Plywoods

by Vibration Method. Mokuzai Gakkaishi. 1992; 38(10): 895–902.
24. Nakao T, Okano T, Asano I. Vibrational properties of a wooden plate. Mokuzai Gakkaishi. 1985; 31(10): 793–800.
25. Zhou J, Chui YH, Gong M, et al. Comparative study on measurement of elastic constants of wood-based panels using modal testing: choice of boundary conditions and calculation methods. Journal of Wood Science. 2017; 63(5): 523–538. doi: 10.1007/s10086-017-1645-0
26. He L, Liang Y, Zhang L, et al. Measurement and Analysis of the Vibration Responses of Piano Soundboards with Different Structures. Materials. 2024; 17(5): 1004. doi: 10.3390/ma17051004
27. Amabili M. Vibrations of rectangular plates. In: Nonlinear Vibrations and Stability of Shells and Plates. Cambridge University Press; 2008. pp. 120–140.
28. Nakao T, Okano T, Asano I. Vibrational properties of a wooden plate. Mokuzai Gakkaishi, 1985, 31(10): 793-800. Available online: https://www.kaiseisha-press.ne.jp/catalogue/ISBN4-86099-905-3sample/cgi-bin/db.cgi?type=searchcard&rec=5&begin=0&word=%22vibrational+properties%22&line=20&d_mode=en&display=en
29. Zhai X, Wang J, Cheng X, et al. Noise Separation Techniques for Accurate Substation Anomaly Detection: An Intelligent Methodology. HighTech and Innovation Journal. 2025; 6(4): 1465–1485. doi: 10.28991/HIJ-2025-06-04-020
30. Han J. Improved Skyline-BP Network for Multi-Track MIDI Music Melody Extraction and Style Classification. HighTech and Innovation Journal. 2025; 6(4): 1170–1184. doi: 10.28991/HIJ-2025-06-04-04